Inorganica Chimica Acta, 177 (1990) 267–275

The synthesis, molecular structure and magnetic properties of $[Ni_2L(\mu\text{-}Cl)Cl_2(H_2O)_2]\cdot 2H_2O\cdot(C_2H_5OH)_{0.42}$ and $[Co_2L(\mu\text{-}Cl)Cl_2]\cdot(H_2O)_{0.18}$ (L = 2,6-bis-(*N*,*N*'-dimethylethylenenamineformidoyl)-4-methylphenolato)

Estelle R. Quijano, Edwin D. Stevens and **Charles J. O'Connor***

Department of Chemistry, University of New Orleans, New Orleans, LA 70148 (U.S.A.)

(Received April 2, 1990; revised July 5, 1990)

Abstract

The crystal structure and magnetic properties of nickel(II) and cobalt(II) binuclear complexes are reported. The nickel(II) and cobalt(II) binuclear molecules consist of a large binucleating ligand, 2,6-bis-(*N*,*N*'-dimethylethylenenamineformidoyl)-4-methylphenolato, and a small exogenous bridging anion, Cl^-. The Curie–Weiss parameters are $C = 2.29$ emu-K/mol, $\theta = +1.7$ K, for the nickel complex and $C = 5.79$ emu-K/mol, $\theta = +10.3$ K for the cobalt complex. The magnetic coupling parameters in both the nickel(II) and the cobalt(II) analogs are consistent with ferromagnetic exchange between the two metal(II) centers and fits of the data with binuclear magnetic exchange models give ferromagnetic coupling parameters of $J/k = +3.6$ and $+9.5$ K for the nickel(II) and cobalt(II), respectively. Crystal data: $[Ni_2(C_{17}H_{28}N_4O)(\mu\text{-}Cl)Cl_2(H_2O)_2]\cdot 2H_2O\cdot(C_2H_5OH)_{0.42}$, $M_r = 619.55$ g/mol, space group $C222_1$, $a = 10.262(4)$, $b = 24.691(4)$, $c = 11.632(4)$ Å, $V = 2947.3$ Å^3, $Z = 4$, $D_x = 1.396$ g/cm^3, λ(Mo Kα) = 0.71073 Å, $\mu = 15.93$ cm^{-1}, $F(000) = 1295.7$, $T = 100$ K, $R = 5.8\%$, $R_w = 9.0\%$ with 1134 unique observed reflections; $[Co_2(C_{17}H_{28}N_4O)(\mu\text{-}Cl)Cl_2]\cdot(H_2O)_{0.18}$, $M_r = 531.90$ g/mol, space group $C2/c$, $a = 10.488(3)$, $b = 24.505(7)$, $c = 26.501(7)$ Å, $\beta = 99.89(2)°$, $V = 6714.3$ Å^3, $Z = 12$, $D_x = 1.578$ g/cm^3, $\lambda = 0.71073$ Å, $\mu = 18.58$ cm^{-1}, $F(000) = 3273.6$, $T = 120$ K, $R = 2.9\%$, $R_w = 3.9\%$ with 2455 observed unique reflections.

Introduction

There have been several reports published in which copper(II) dinuclear complexes have been studied that have the general structure as shown in **1**.

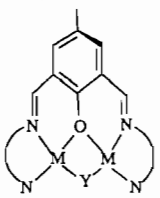

1

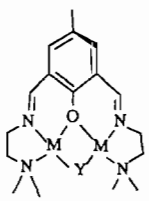

2

The bridging pathways consist of an endogenous phenoxide bridge contained in the binucleating ligand, and a smaller exogenous bridging ligand (Y). Several copper(II) binuclear complexes of type **1** have been reported [1–9] that contain a variety of dissimilar bridging pathways, including $Y = Cl^-$ [4], Br^- [5], OH^- [6–8], 1,1-N_3^- [9] and others. These copper binuclear molecules are of interest in part because they are potential models for the metabolic copper protein hemocyanin. The modeling interest in these copper(II) binuclears is primarily due to the fact that these model compounds emulate the coordination environment and magnetic properties of blue copper proteins [2, 4, 10–12].

We have expanded our research on compounds of general formula **1** to include the examination of complex **2** containing transition metals other than copper(II). The two complexes involved in the present study are obtained by exchanging the copper(II) ions for either nickel(II) or cobalt(II) ions. Both binuclear molecules still incorporate a small molecule into the bridging cavity (Cl^-). The Ni^{2+} ion in the $[Ni_2L(\mu\text{-}Cl)Cl_2(H_2O)_2]\cdot 2H_2O\cdot(C_2H_5OH)_{0.42}$ complex exhibits normal Curie–Weiss paramagnetism at high temperatures. At the lowest temperatures, zero field splitting and binuclear ferromagnetic coupling are detected in the magnetic susceptibility data. The geometric analog, $[Co_2L(\mu\text{-}Cl)Cl_2]\cdot(H_2O)_{0.18}$, exhibits Curie–Weiss behavior at high temperatures, with a ferromagnetic Weiss constant. This behavior is indicative of ferromagnetic exchange between the two cobalt(II) ions in the binuclear molecule. We

*Author to whom correspondence should be addressed.

0020-1693/90/$3.50

report here on the synthesis, crystal structures and magnetic properties of the two binuclear transition metal complexes $[Ni_2L(\mu\text{-}Cl)Cl_2(H_2O)_2]\cdot 2H_2O\cdot(C_2H_5OH)_{0.42}$ and $[Co_2L(\mu\text{-}Cl)Cl_2]\cdot(H_2O)_{0.18}$.

Experimental

Synthesis

2-Formidoyl-4-methylsalicylaldimine (FSAL)

FSAL was obtained from Trans World Chemicals and recrystallized from absolute ethanol at 70 °C.

$[Ni_2L(\mu\text{-}Cl)Cl_2(H_2O)_2]\cdot 2H_2O\cdot(C_2H_5OH)_{0.42}$

One mmol of FSAL was dissolved in 10 ml of 95% ethanol. To this was added 1 mmol of dimethylethylenediamine and 2 mmol of $NiCl_2$ previously dissolved by heating at 70 °C in ~5 ml of 95% ethanol. After stirring thoroughly, the solution was filtered by suction and washed with methanol, the remaining filtrate was allowed to stand. After a few days, large bright green crystals appeared. They were slightly soluble in ethanol. The crystals were recovered by decanting off most of the solution. Several trials were made in order to grow crystals of a suitable nature for X-ray diffraction studies. The crystals were often twinned as a result of growing in layers into a block-shaped structure. Crystals of the best size and shape were formed when a few hundredths of a gram of excess FSAL was added to a saturated solution of the complex in absolute ethanol along with a few drops of triethylorthoformate to scavenge for excess water. Crystals were observed to decompose on standing due to solvent evaporation. This was kept to a minimum by storing the crystals in the presence of a small amount of the mother liquor.

$[Co_2L(\mu\text{-}Cl)Cl_2]\cdot(H_2O)_{0.18}$

One mmol of FSAL was dissolved in 10 ml of absolute ethanol. To this was added 1 mmol of dimethylethylenediamine and three drops of triethylorthoformate. This was heated to 70 °C. A separate solution made from 2 mmol of anhydrous $CoCl_2$ which was dissolved in ~5 ml acetonitrile that had been dried over acid wash was heated and then added to the FSAL solution. After the solution had been filtered by suction, the remaining solvent was separated into three test tubes and allowed to stand in a sulfuric acid desiccator for several days. Crystalline material was recovered from these test tubes and washed with dry acetonitrile. The crystals recovered were opaque, shiny, greenish-black, and rectangular in shape.

Magnetism

The magnetic susceptibility was measured with a superconducting SQUID susceptometer in a temperature region of 6–350 K. The materials exhibited solvent evaporation and decomposition when heated above 300 K, so only the data between 6–300 K is reported. Measurement of this data and calibration procedures have been reported previously [13]. See also 'Supplementary material'.

Crystallographic studies

A single crystal of the nickel complex with approximate dimensions of $0.4\times0.4\times0.15$ mm was mounted on an Enraf-Nonius CAD-4 four circle diffractometer. The sample was cooled to approximately 100 K using a stream of cold nitrogen gas generated by a locally modified Enraf-Nonius low temperature device. The cell dimensions were determined by least-squares refinement of the measured setting angles of 25 reflections with $40°\leqslant 2\theta\leqslant 50°$. The space group was determined by searching for systematically absent reflections and later confirmed by successful solution of the structure. The systematic absences hkl: $h+k=2n+1$ and $00l$: $l=2n+1$ and orthorhombic lattice type indicated the space group $C222_1$ (No. 21). Crystal data are summarized in Table 1.

Integrated intensity measurements were collected in the $\omega{:}2\theta$ scan mode with a graphite crystal monochromator and a molybdenum target X-ray tube. During data collection, three standard reflections were monitored every 2 h for changes in intensity, and three high angle reflections were recentered after every 200 reflections measured to check for changes in crystal orientation. The standard reflections showed variations of less than 0.6% during data collection. Empirical absorption corrections were applied based on observations of the intensities of the two reflections as a function of rotation of ψ about the scattering vector. The data were then corrected for Lorentz and polarization effects. A total of 1296 reflections was measured yielding a final set of 1134 reflections with $I>3\sigma(I)$.

The structure was solved by direct methods using the program MULTAN80 [14]. The metal and halogen atoms were located in the initial E-maps, and successive Fourier syntheses alternated with least-squares full matrix refinements revealed the positions of all non-hydrogen atoms. In addition to the $[Ni_2L(\mu\text{-}Cl)Cl_2(H_2O)_2]$ molecule located on a crystallographic two-fold axis, an additional water molecule and a partially occupied disordered ethanol molecule were located in subsequent difference Fourier summation maps. The function $S=\Sigma w(|F_o|-|F_c|)^2$ was minimized

TABLE 1. Crystal and data collection parameters

	I	II
Formula	$[Ni_2L(\mu\text{-}Cl)Cl_2(H_2O)_2]\cdot 2H_2O\cdot(C_2H_5OH)_{0.42}$	$[Co_2L(\mu\text{-}Cl)Cl_2]\cdot(H_2O)_{0.18}$
a (Å)	10.262(4)	10.495(3)
b (Å)	24.691(4)	24.506(7)
c (Å)	11.632(4)	26.501(7)
α (°)	90.0	90.0
β (°)	90.0	99.89(2)
γ (°)	90.0	90.0
V (Å^3)	2947.3(16)	6714.5(32)
Crystal system	orthorhombic	monoclinic
Z	4	12
Space group	$C222_1$	$C2/c$
M_r (g mol^{-1})	619.55	531.90
T (K)	100(5)	120(5)
μ (cm^{-1})	15.93	18.58
Crystal decay (%)	0.6	4.0
$F(000)$	1295.7	3273.6
λ (Å)	0.71073	0.71073
Crystal color	emerald	black
Crystal habit	cubic	irregular
Crystal size (mm)	0.4×0.4×0.15	0.2×0.2×0.1
D_{calc} (g/cm^3)	1.396(5)	1.578(5)
$(\sin\theta/\lambda)_{max}$ (Å^{-1})	0.59	0.48
2λ limits (°)	$5<2\theta<45$	$5<2\theta<40$
Transmission (%) max.	99.7	99.9
min.	77.5	87.3
Range h (max., min.)	0, 12	0, 10
k	0, 29	0, 23
l	0, 13	−25, 25
No. unique reflections	1296	3206
No. observed reflections	1134	2455
Criteria unobserved reflections	$I_o<3\sigma I_o$	$I_o<3\sigma I_o$
Unobserved reflections	162	740
R (%)[a]	5.8	2.9
R_w (%)[a]	9.0	3.9
$(\Delta/\sigma)_{max}$	0.01	0.01
$(\Delta\rho)_{max}$ (e/Å^3)	1.1	3.3

[a] $R=\Sigma w(|F_o|-|F_c|)/\Sigma w|F_o|$; $R_w=[\Sigma w(|F_o|-|F_c|)^2/\Sigma wF_o^2]^{1/2}$.

where $w=1/(\sigma(F_o))^2$. Standard deviations were estimated by $\sigma(F_o^2)=((\sigma_{cs})^2+(0.04F_o^2)^2)^{1/2}$ where σ_{cs} represents the contribution from counting statistics. Hydrogen atom positions on the ligand L were calculated and included with fixed positions and isotropic thermal parameters. Hydrogen atoms bonded to the water oxygens were located in the difference Fourier synthesis and included with fixed positions and isotropic thermal parameters. Anisotropic thermal parameters were refined for all other atoms except those in the disordered ethanol molecule which were refined isotropically. The disordered ethanol is located within 0.5 Å of the two-fold axis. Since both the ethanol molecule and its equivalent generated by the two-fold axis cannot simultaneously occupy the site in the lattice, the maximum occupancy factor for the ethanol is 0.5. When a common occupancy factor for the three atoms of the ethanol molecule was included as a variable in the least-squares refinement, an occupancy of 0.42(1) was obtained. Comparison of the magnitudes of F_o and F_c for the largest structure factors indicated the presence of a minor secondary extinction effect, and an isotropic extinction parameter was included in the refinement. Reflections where I_o was less than $3\sigma(I_o)$ were considered 'unobserved' and were not included in the refinement. Computer programs used in data collection, reduction and refinement are a part of the CAD4SDP package [15]. Atomic scattering factors and anomalous dispersion corrections for Ni, Cl, O, N and C were taken from the International Tables of X-ray Crystallography [16].

The structure of the cobalt complex was determined by the same procedure as the nickel complex except

as noted below. A single crystal with approximate dimensions 0.2×0.2×0.1 mm was mounted on the diffractometer and cooled to 120 K. Systematic absences *hkl*: $h+k=2n+1$ and *h0l*: $l=2n+1$ and monoclinic lattice type indicated either the *Cc* or *C2/c* space group. Space group *C2/c* was chosen on the basis of intensity statistics and confirmed by the successful structure determination. The standard reflections showed a gradual decay of 4% during data collection, and a linear least-squares fit to their intensities was used to correct the data. A total of 3206 reflections was measured yielding a final set of 2455 observed reflections.

The structure was solved by direct methods yielding positions of all the heavy atoms in the initial *E*-map. The asymmetric unit contains 1.5 $Co_2L(\mu\text{-}Cl)Cl_2$ molecules: one molecule in a general position and one half-molecule located on a crystallographic two-fold axis. A partially occupied water oxygen also located on the two-fold axis was found in a difference Fourier synthesis. Hydrogen atom positions on the ligand L were calculated and included as fixed contributions to the refinement. The hydrogen atoms on the water molecule were not located. No significant secondary extinction effects were observed in the data.

Results and discussion

The 2,6-bis-(*N*,*N'*-dimethylethyleneamineformidoyl)-4-methylphenolato) ligand is pentadentate and capable of binding two transition metal ions in close proximity. The possibility of forming bonds from the metal ions to axial or bridging ligands above, below, and in the plane generates a large number of coordination geometries. Except for the dimethylaminoethane side chains, the ligand is highly planar. The bond angles and bond lengths within this ligand in both the Ni and Co complexes are similar to the observed binuclear Cu^{II} complexes of 2,6-bis-(*N*-2-pyridylformidolyl)-4-methylphenol [5, 17].

The $[Ni_2L(\mu\text{-}Cl)Cl_2(H_2O)_2]\cdot 2H_2O\cdot(C_2H_5OH)_{0.42}$ complex sits on a two-fold rotation axis passing through the center of the molecule at the phenoxide bridge. The Ni···Ni distance is 3.187(2) Å. An ORTEP diagram of the $[Ni_2L(\mu\text{-}Cl)Cl_2(H_2O)_2]$ binuclear unit is illustrated in Fig. 1. (Figure S1 illustrates the packing diagram of the unit cell.) A Cl(1) ion also sits on the two-fold axis and occupies the in-plane bridging position between the two Ni atoms. Both Ni atoms are also coordinated to a Cl(2) ion and a water molecule. This is in agreement with nickel's propensity to form stable, six-coordinate species. The axial bonds, Ni(1)–O(2) (2.207(5) Å) and Ni(1)–Cl(2) (2.421(3) Å) are slightly elongated

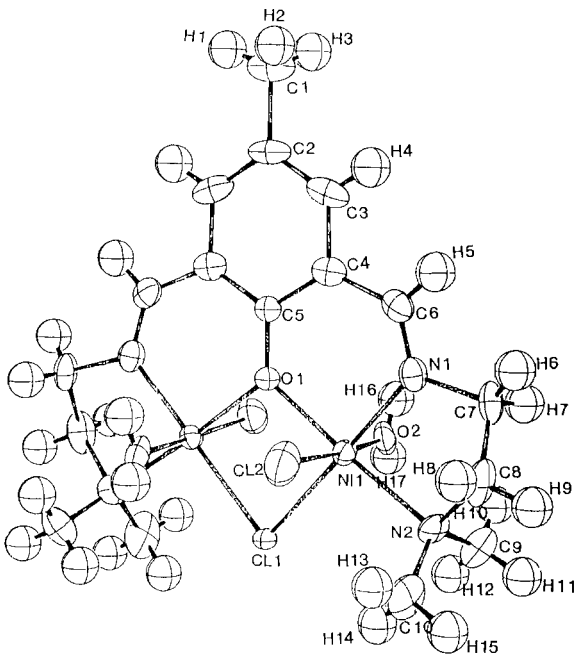

Fig. 1. ORTEP diagram of the binuclear $[Ni_2L(\mu\text{-}Cl)Cl_2(H_2O)_2]$ unit of $[Ni_2L(\mu\text{-}Cl)Cl_2(H_2O)_2]\cdot 2H_2O\cdot(C_2H_5OH)_{0.42}$ crystalline material.

compared to the in-plane distances Ni(1)–O(1) (2.028(3) Å) and Ni(1)–Cl(1) (2.387(2) Å). The final positional parameters for nickel are listed in Table 2. Bond distances and angles are listed in Tables 3 and 4, respectively. (The contents of the unit cell are plotted in Fig. S1.) The water molecule coordinated to the nickel atom forms hydrogen bonds to the oxygen of the ethanol molecule, O(2)···O(4) (2.60(2) Å), and to the uncoordinated water molecule, O(2)···O(3) (2.940(6) Å). The uncoordinated water molecule is also hydrogen bonded to an equivalent water molecule generated by the two-fold axis, O(3)···O(3) (2.816(8) Å), and to the axial Cl ion, O(3)···Cl(2) (3.171(5) Å).

The $[Co_2L(\mu\text{-}Cl)Cl_2]\cdot(H_2O)_{0.18}$ complex contains one and a half molecules per asymmetric unit, with one molecule at a general position and one sitting on a two-fold axis similar to the nickel complex (Fig. S2). In both molecules the cobalt atoms are in a coordination geometry which is intermediate between five-coordinate square pyramidal and trigonal bipyramidal. For convenience, the square pyramidal geometry is assumed for the purposes of discussion. In the half molecule, the axial Co–Cl distance, Co(1)–Cl(2) (2.287(1) Å) is shorter than the equatorial distance, Co(1)–Cl(1) (2.378(1) Å). The other molecule in the unit cell lacking a two-fold axis (Fig. 2) generates four different Co–Cl distances, two from the bridging Cl(3) ion, Co(2)–Cl(3) (2.391(1) Å) and Co(3)–Cl(3) (2.398(1) Å), and two others from the

TABLE 2. Positional parameters and their e.s.d.s.

Atom	x	y	z	B (Å^2)
Ni1	0.3693(1)	0.34349(5)	0.1760(1)	1.83(2)
Cl1	0.500	0.4155(2)	0.250	2.67(8)
Cl2	0.2441(5)	0.3379(2)	0.3521(4)	6.2(1)
O1	0.500	0.2927(4)	0.250	1.9(2)
O2	0.4994(8)	0.3446(3)	0.0250(6)	3.1(2)
O3	0.0934(6)	0.2260(3)	0.3387(6)	1.4(1)
O4	0.397(4)	0.422(2)	0.596(3)	3.0(7)*
N1	0.2745(9)	0.2824(4)	0.1080(8)	2.5(2)
N2	0.2204(9)	0.3917(4)	0.0969(9)	2.5(2)
Cl	0.500	0.0618(7)	0.250	4.0(4)
C2	0.500	0.1234(6)	0.250	3.2(4)
C3	0.406(1)	0.1518(4)	0.1945(9)	3.0(2)
C4	0.406(1)	0.2095(4)	0.1905(9)	2.3(2)
C5	0.500	0.2396(6)	0.250	1.9(3)
C6	0.296(1)	0.2322(5)	0.126(1)	2.7(2)
C7	0.160(1)	0.2987(5)	0.036(1)	2.9(3)
C8	0.114(1)	0.3515(6)	0.082(1)	3.7(3)
C9	0.259(1)	0.4137(6)	−0.014(1)	4.0(3)
C10	0.179(1)	0.4345(6)	0.169(2)	5.1(4)
C11	0.421(8)	0.387(3)	0.706(7)	5.0(9)*
C12	0.427(5)	0.426(2)	0.724(4)	3.2(8)*

Starred atoms were refined isotropically. Anisotropically refined atoms are given in the form of the isotropic equivalent thermal parameter defined as: $B_{eq} = (4/3)[a^2\beta_{1,1} + b^2\beta_{2,2} + c^2\beta_{3,3} + ab(\cos\gamma)\beta_{1,2} + ac(\cos\beta)\beta_{1,3} + bc(\cos\alpha)\beta_{2,3}]$.

axial, out of plane Cl(4) and Cl(5) distances Co(2)–Cl(4) (2.288(1) Å) and Co(3)–Cl(5) (2.296(1) Å). In the half molecule O(1), Cl(1), N(1) and N(2) occupy equatorial positions. The other molecule containing Co(2) and Co(3) has two square pyramidal planes with equatorial positions: N(3), O(2), Cl(3) and N(4) for Co(2); O(2), Cl(3), N(5) and N(6) for Co(3). The Co(1)···Co(1) distance is 3.236(1) Å and the Co(2)···Co(3) distance is 3.241(1) Å. The final positional parameters are given in Table 5. Bond distances and angles for the cobalt complex are listed in Tables 6 and 7, respectively. (Figure S3 illustrates the packing diagram of the unit cell.) The molecules located on the two-fold axis are linked by the hydrogen bonds between the axial Cl ion and the partially occupied water molecule also on a two-fold axis, O(3)···Cl(2) (3.348(5) Å). Thus, the alternating water and Co complexes form a hydrogen-bonded linear chain propagating in the crystallographic a direction.

The effective magnetic moment ($\mu_{eff} = \sqrt{7.997\ \chi T}$) for the nickel(II) analog is plotted as a function of temperature and is shown in Fig. 3. At higher temperatures, Curie–Weiss behavior is observed for the complex as expected for a six coordinate, octahedral Ni^{2+} ($3d^8$) species. The Curie–Weiss law expression is illustrated in eqn. (1).

$$\chi = \frac{C}{T-\theta} = \frac{Ng^2\mu_B{}^2S(S+1)}{3k(T-\theta)} \quad (1)$$

The temperature dependent magnetic susceptibility data for the nickel(II) complex was fit with the Curie–Weiss equation and gave the best fit parameters: $C = 2.29$ emu-K/mol(Ni_2), $\theta = 1.72$ K. For Ni^{+2} with $S = 1$ and $3d^8$ electron structure, the Curie constant corresponds to a g value of 2.13.

The fitted parameters imply that there is a small ferromagnetic exchange propagated through the bridging pathways. An inspection of the behavior of the effective magnetic moment plotted as a function of temperature shows a maximum at the lowest temperatures. This is consistent with a ferromagnetic *intra*-binuclear interaction plus a spin coupling interaction accomplished either through *inter*-binuclear interactions or through the action of zero field splitting that is allowed for spin $S = 1$ systems.

The spin Hamiltonian that best describes the possible interactions that may occur in a nickel(II) binuclear molecule is given in eqn. (2)

$$\mathcal{H} = -2JS_1S_2 - D(S_{1z}{}^2 + S_{2z}{}^2) - g\mu_B HS \quad (2)$$

TABLE 3. Bond distances (Å)

Atom 1	Atom 2	Distance	Atom 1	Atom 2	Distance
Ni1	Cl1	2.387(2)	N1	C7	1.502(9)
Ni1	Cl2	2.421(3)	C4	C5	1.403(8)
Ni1	O1	2.028(3)	N2	C8	1.489(10)
N2	C9	1.455(10)	C4	C6	1.462(11)
Ni1	O2	2.207(5)	N2	C10	1.419(11)
Ni1	N1	1.962(6)	C1	C2	1.520(13)
Ni1	N2	2.144(6)	C3	C4	1.425(9)
C2	C3	1.359(9)	C7	C8	1.483(11)
O1	C5	1.312(10)	C11	C12	0.97(5)
O4	C11	1.56(5)	N1	C6	1.277(9)

Numbers in parentheses are e.s.d.s. in the least significant digits.

TABLE 4. Bond angles (°)

Atom 1	Atom 2	Atom 3	Angle	Atom 1	Atom 2	Atom 3	Angle
Cl1	Ni1	Cl2	92.05(7)	C9	N2	C10	109.3(7)
Cl1	Ni1	O1	86.3(1)	C1	C2	C3	121.1(4)
Cl1	Ni1	O2	86.4(1)	N2	C8	C7	113.3(6)
Cl1	Ni1	N1	175.3(2)	C8	N2	C9	110.1(7)
Cl1	Ni1	N2	98.2(2)	C8	N2	C10	110.2(6)
Cl2	Ni1	O1	87.52(7)	C3	C2	C3	117.8(9)
Cl2	Ni1	O2	174.3(1)	Ni1	N2	C10	111.9(5)
Cl2	Ni1	N1	92.0(2)	N1	C6	C4	126.1(7)
Cl2	Ni1	N2	91.0(2)	Ni1	N1	C7	114.1(4)
O1	Ni1	O2	86.8(1)	C6	N1	C7	119.2(6)
O1	Ni1	N1	91.4(2)	Ni1	N2	C9	113.2(5)
O1	Ni1	N2	175.3(2)	O4	C11	C12	101(3)
O2	Ni1	N1	89.3(2)	C2	C3	C4	122.1(7)
O2	Ni1	N2	94.7(2)	C3	C4	C6	113.5(7)
N1	Ni1	N2	84.3(3)	N1	C7	C8	106.6(6)
Ni1	Cl1	Ni1	83.76(8)	N2	C7	C6	111.2(3)
Ni1	O1	Ni1	103.6(3)	Ni1	N2	C8	101.9(4)
Ni1	O1	C5	128.2(1)	Ni1	N1	C6	126.4(5)

Numbers in parentheses are e.s.d.s. in the least significant digits.

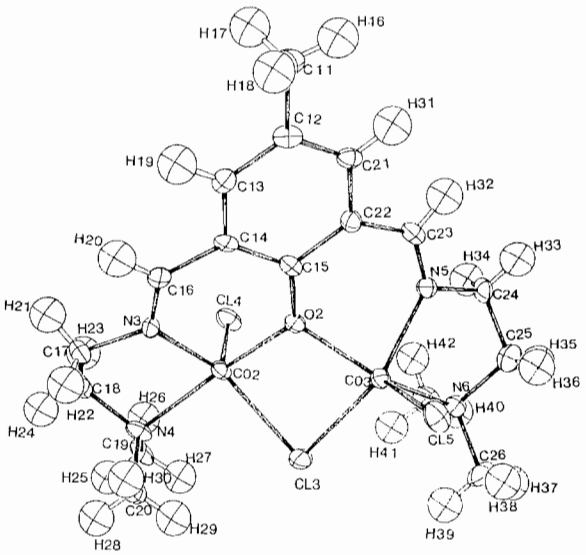

Fig. 2. ORTEP diagram of the molecule $Co_2L(\mu\text{-}Cl)Cl_2$ unit of the $Co_2L(\mu\text{-}Cl)Cl_2 \cdot (H_2O)_{0.18}$ crystalline material.

The D term represents the usual zero field splitting of the $^3A_2$ ground state of nickel(II), with the sign convention that a positive D corresponds to the doublet being below the singlet. The expression for the magnetic susceptibility derived from this spin Hamiltonian has been reported [18] and is so lengthy that it will not be reproduced here. We refer to this equation as $\chi(g, J, D)$.

In our analysis, we have allowed for an *inter*-dimer exchange term through the addition of the molecular field exchange approximation [13] which yields the exchange corrected susceptibility as

$$\chi(g, J, D, zJ') = \frac{\chi(g, J, D)}{1 - \left(\frac{zJ'}{Ng^2\mu_B{}^2}\right)\chi(g, J, D)} + TIP \quad (3)$$

The magnetic susceptibility data was fit to eqn. (3) and is illustrated as the smooth line drawn through the effective magnetic moment data points as shown in Fig. 3. All of the parameters were allowed to vary freely and the best fitted parameters are: $g = 2.06$, $J/k = 3.6$ K, $D/k = 7.1$ K, $zJ'/k = -0.6$ K, $TIP = 0.001$ emu/mol. All of the parameters are reasonable for a $3d^8$ nickel(II) system, and indicate that there is a weak ferromagnetic interaction between the two Ni^{+2} centers of the binuclear molecule. However, this interaction is tempered by the zero field splitting that is commonly found to occur in a magnetic ion with spin quantum number $S = 1$. The values of zJ' and D are not independent. The effect on the calculated magnetic susceptibility caused by a small variation of zJ' may be compensated for by a corresponding variation of D over a limited range, without affecting the quality of the fit. Therefore the significance of D and zJ' as independent parameters should be viewed with caution. Nevertheless, the value of the primary exchange term J is unambiguous and represents an accurate measure of the *intra*-binuclear magnetic coupling in this complex.

The inverse magnetic susceptibility of the cobalt analog, $[Co_2L(\mu\text{-}Cl)Cl_2] \cdot (H_2O)_{0.18}$, is plotted as a function of temperature in Fig. 4. The plot is linear and indicates that Curie–Weiss law is being followed at high temperatures. The cobalt analog was fit to the Curie–Weiss law (eqn. (1)) over the 50–300 K

TABLE 5. Positional parameters and their e.s.d.s.

Atom	x	y	z	B (Å^2)
Co1	0.14485(5)	0.38409(2)	0.73675(2)	1.31(1)
Co2	0.54436(6)	0.31889(2)	0.51993(2)	1.39(1)
Co3	0.54453(6)	0.38303(2)	0.41297(2)	1.38(1)
Cl1	0.000	0.31300(7)	0.750	2.96(4)
Cl2	0.3078(1)	0.39585(5)	0.80516(5)	2.40(3)
Cl3	0.4891(1)	0.29137(5)	0.43232(4)	2.07(3)
Cl4	0.3628(1)	0.35536(5)	0.54364(5)	2.17(3)
Cl5	0.7086(1)	0.38195(5)	0.36574(5)	2.23(3)
O1	0.000	0.4337(2)	0.750	1.62(9)
O2	0.6185(3)	0.3849(1)	0.4884(1)	1.45(7)
O3	0.500	0.4774(4)	0.750	4.00(2)*
N1	0.1936(3)	0.4427(1)	0.6892(1)	1.54(8)
N2	0.2462(3)	0.3348(2)	0.6901(1)	1.63(8)
N3	0.7028(3)	0.3212(1)	0.5759(1)	1.43(8)
N4	0.5314(3)	0.2377(1)	0.5509(1)	1.77(8)
N5	0.5225(3)	0.4655(1)	0.4202(1)	1.41(8)
N6	0.3851(3)	0.3957(2)	0.3523(1)	1.65(8)
C1	0.000	0.6649(3)	0.750	2.7(2)
C2	0.000	0.6043(3)	0.750	1.7(1)
C3	0.0797(4)	0.5752(2)	0.7236(2)	1.5(1)
C4	0.0836(4)	0.5181(2)	0.7235(2)	1.4(1)
C5	0.000	0.4881(3)	0.750	1.3(1)
C6	0.1724(4)	0.4937(2)	0.6933(2)	1.4(1)
C7	0.2848(4)	0.4252(2)	0.6560(2)	2.1(1)
C8	0.3456(4)	0.3725(2)	0.6763(2)	1.9(1)
C9	0.3112(5)	0.2876(2)	0.7178(2)	3.0(1)
C10	0.1600(5)	0.3147(2)	0.6440(2)	2.9(1)
C11	0.9940(5)	0.5404(2)	0.5746(2)	2.4(1)
C12	0.8886(4)	0.4999(2)	0.5537(2)	1.5(1)
C13	0.8801(4)	0.4488(2)	0.5760(2)	1.5(1)
C14	0.7873(4)	0.4105(2)	0.5567(2)	1.3(1)
C15	0.6991(4)	0.4221(2)	0.5112(2)	1.3(1)
C16	0.7841(4)	0.3602(2)	0.5852(2)	1.5(1)
C17	0.7155(5)	0.2745(2)	0.6111(2)	2.0(1)
C18	0.5876(5)	0.2457(2)	0.6057(2)	2.0(1)
C19	0.3991(5)	0.2162(2)	0.5456(2)	2.9(1)
C20	0.6096(5)	0.1992(2)	0.5264(2)	2.4(1)
C21	0.7931(4)	0.5133(2)	0.5136(2)	1.6(1)
C22	0.6993(4)	0.4763(2)	0.4913(2)	1.3(1)
C23	0.5989(4)	0.4960(2)	0.4503(2)	1.5(1)
C24	0.4200(4)	0.4901(2)	0.3827(2)	1.8(1)
C25	0.3961(4)	0.4531(2)	0.3364(2)	2.1(1)
C26	0.3884(5)	0.3591(2)	0.3082(2)	2.7(1)
C27	0.2629(5)	0.3869(2)	0.3720(2)	2.7(1)

Starred atoms were refined isotropically.

TABLE 6. Bond distances (Å)

Atom 1	Atom 2	Distance	Atom 1	Atom 2	Distance
Co1	Cl1	2.378(1)	C2	C3	1.379(5)
N6	C25	1.479(5)	C3	C4	1.400(5)
Co1	Cl2	2.287(1)	C4	C5	1.419(5)
O1	C5	1.332(6)	N6	C26	1.477(5)
Co1	O1	2.024(2)	N6	C27	1.481(6)
C1	C2	1.484(8)	C4	C6	1.457(5)
Co1	N1	2.034(3)	C7	C8	1.498(6)
Co1	N2	2.137(3)	O2	C15	1.319(4)
Co2	Cl3	2.391(1)	C11	C12	1.517(6)
Co2	Cl4	2.288(1)	N1	C6	1.276(5)
Co2	O2	2.036(2)	N1	C7	1.471(5)
Co2	N3	2.030(3)	C12	C21	1.370(5)
Co2	N4	2.164(3)	N2	C8	1.487(5)
Co3	Cl3	2.398(1)	N2	C9	1.472(5)
Co3	Cl5	2.296(1)	N2	C10	1.476(6)
Co3	O2	2.016(3)	C12	C13	1.394(6)
Co3	N5	2.046(3)	N3	C16	1.276(5)
Co3	N6	2.135(3)	N3	C17	1.471(5)
C13	C14	1.386(6)	C14	C15	1.416(5)
N4	C18	1.485(5)	C14	C16	1.450(6)
N4	C19	1.470(5)	C15	C22	1.429(5)
N4	C20	1.473(5)	C17	C18	1.501(6)
N5	C23	1.273(5)	C22	C23	1.460(6)
N5	C24	1.463(5)	C24	C25	1.512(6)
C21	C22	1.392(5)			

Numbers in parentheses are e.s.d.s. in the least significant digits.

temperature region, and gave the best fitted parameters for the binuclear unit of $C = 5.79$ emu-K/mol and $\theta = 10.3$ K.

From the high temperature Curie–Weiss fit, it is evident that the cobalt complex exhibits moderate ferromagnetic coupling between the two cobalt(II) ions. The analysis of the cobalt(II) ion is complicated by the fact that there is a great deal of distortion in the molecular geometry of the cobalt(II) ion. The magnetic susceptibility behavior is affected by unquenched angular momentum that arises from the ^{4}F ground term of the $3d^7$ electronic configuration of cobalt(II). Spin–orbit coupling and a crystal field of low symmetry leads to a complicated splitting of the ^{4}F ground term. However, the action of the crystal field and spin–orbit coupling interactions on the ^{4}F ground term symbol commonly results in a highly anisotropic Kramers doublet ground state, and a lowest excited state some 50 cm^{-1} above the Kramers doublet. We may therefore approximate the behavior of the low temperature magnetic susceptibility data by using a simple spin $S = 1/2$ model if we restrict the data to temperatures below 50 K. The magnetic susceptibility equation that describes the behavior expected for a binuclear $S_1 = S_2 = 1/2$ system is given in eqn. (4).

$$\chi = \frac{2Ng^2\mu_B{}^2}{kT} \frac{e^{2x}}{1+3e^{2x}} \tag{4}$$

where $x = J/kT$ and $2J$ is the separation of the singlet and triplet states with a negative J denoting a ground singlet.

TABLE 7. Bond angles (Å)

Atom 1	Atom 2	Atom 3	Angle	Atom 1	Atom 2	Atom 3	Angle
Cl1	Co1	Cl2	112.65(3)	N5	Co3	N6	80.8(1)
C23	N5	C24	119.5(3)	Co3	N6	C25	105.2(2)
Cl1	Co1	O1	84.05(9)	Cl1	Co1	N1	147.6(9)
Co2	Cl3	Co3	85.19(4)	Co3	N6	C26	112.7(3)
Cl1	Co1	N2	93.74(9)	Co3	N6	C27	109.1(3)
Cl2	Co1	O1	105.56(5)	Co1	O1	C5	126.92(8)
C25	N6	C26	109.82(3)	C26	N6	C27	109.3(3)
Cl2	Co1	N1	99.7(3)	C25	N6	C27	110.7(3)
Cl2	Co1	N2	98.67(9)	Co2	O2	Co3	106.3(1)
O1	Co1	N1	87.7(1)	Co2	O2	Cl5	128.4(2)
O1	Co1	N2	154.59(9)	Co3	O2	C15	125.4(2)
C1	C2	C3	121.2(3)	Co1	N1	C7	115.0(3)
N1	Co1	N2	80.7(1)	Co1	N1	C6	124.9(3)
Cl3	Co2	Cl4	107.60(4)	C2	C3	C4	122.6(4)
Cl3	Co2	O2	82.60(8)	C6	N1	C7	118.6(3)
C3	C4	C5	119.8(4)	C3	C4	C6	115.6(3)
Cl3	Co2	N3	138.47(9)	Co1	N2	C8	103.4(2)
Cl3	Co2	N4	95.04(9)	Co1	N2	C9	113.1(3)
C5	C4	C6	124.6(0)	Co1	N2	C10	111.9(2)
Cl4	Co2	O2	101.40(8)	Cl4	Co2	N3	113.89(9)
C8	N2	C9	109.1(3)	C11	C12	C13	121.9(4)
Cl4	Co2	N4	98.37(9)	C8	N2	C10	111.0(3)
C11	Cl2	C21	121.2(8)	C9	N2	C10	108.3(3)
O2	Co2	N3	87.4(1)	C13	C12	C21	116.9(4)
O2	Co2	N4	159.9(1)	Co2	N3	C16	126.9(3)
C12	C13	C14	123.0(4)	Co2	N3	C17	114.5(3)
N3	Co2	N4	81.2(1)	C13	C14	C15	119.5(4)
Cl3	Co3	Cl5	109.75(4)	C16	N3	C17	118.3(3)
C13	C14	C16	117.5(4)	Co2	N4	C18	102.1(2)
Cl3	Co3	O2	82.84(8)	C15	C14	C16	122.9(4)
Cl3	Co3	N5	150.43(9)	Co2	N4	C19	114.5(2)
C14	C15	C22	117.3(4)	Co2	N4	C20	110.3(2)
Cl3	Co3	N6	96.29(9)	C12	C21	C22	122.9(4)
Cl5	Co3	O2	110.08(8)	C18	N4	C19	110.5(3)
C15	C22	C21	119.6(4)	C18	N4	C20	111.0(3)
Cl5	Co3	N5	99.74(9)	C15	C22	C23	122.4(4)
Cl5	Co3	N6	98.93(9)	C19	N4	C20	108.4(3)
C21	C22	C23	117.8(4)	Co3	N5	C23	124.8(3)
O2	Co3	N5	85.2(1)	O2	Co3	N6	149.5(1)
Co3	N5	C24	115.2(3)				

Numbers in parentheses are e.s.d.s. in the least significant digits.

Following the same procedure used for the nickel analog, we fit eqn. (4), corrected for *inter*-binuclear exchange with the molecular field approximation (eqn. (2)). The best fitted parameters are $g = 6.1$, $J/k = 9.5$ K, and $zJ'/k = -2.5$ K. The large g value arises from the mixing of orbital and spin components in the Kramers doublet and would be expected to be highly anisotropic. The exchange parameter is in reasonable agreement with that predicted by the high temperature Curie–Weiss fit. The molecular exchange term is necessary because of the drop in the magnetic moment at the lowest temperatures. This antiferromagnetic interaction most likely arises from magnetic super-exchange between the neighboring binuclear units and is consistent with the one dimensional hydrogen bonded super-exchange pathway that is observed in the crystal structure determination.

We are continuing our investigation of exchange mechanisms in binuclear molecules with exogenous bridging ligands through the investigation of complexes of cobalt(II) and nickel(II) with bridging

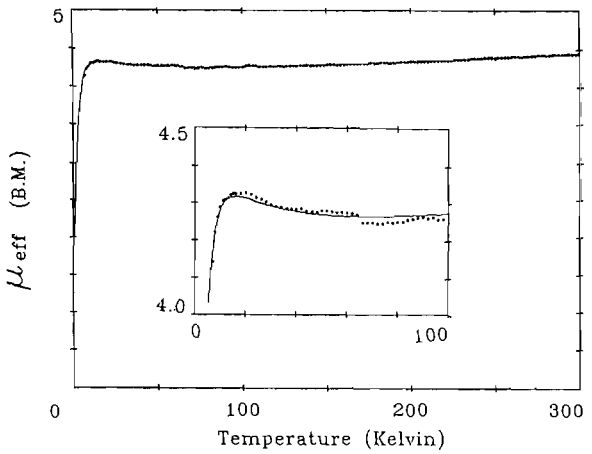

Fig. 3. The effective magnetic moment of $[Ni_2L(\mu\text{-}Cl)Cl_2(H_2O)_2]\cdot 2H_2O\cdot(C_2H_5OH)_{0.42}$ plotted as a function of temperature. The smooth curve drawn through the data points is the best fit of the data as described in the text. The inset shows an expansion of the low temperature region.

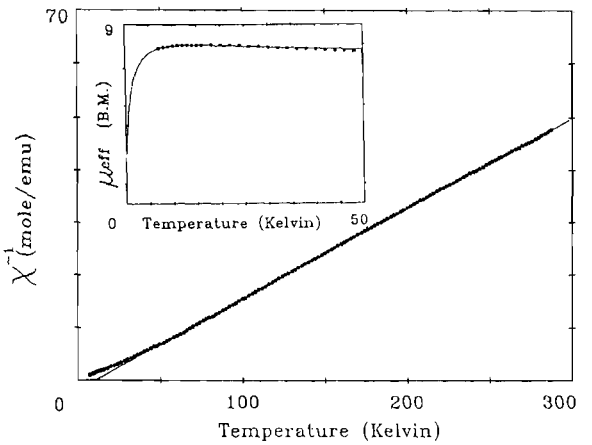

Fig. 4. The inverse magnetic susceptibility of $Co_2L(\mu\text{-}Cl)Cl_2\cdot(H_2O)_{0.18}$ plotted as a function of temperature. The smooth line drawn through the data points is the best fit of the Curie–Weiss law to the data. The inset illustrates the effective magnetic moment plotted as a function of temperature over the 6–50 K temperature region. The curve drawn through the data points in the inset illustrate the best fit of the binuclear model to the data as described in the text.

ligands other than chlorine, for example bromine, iodine, hydroxide and others. We are also extending the investigation to other metals such as manganese and chromium. These investigations will be the topic of future reports.

Supplementary material

Anisotropic thermal parameters for non-hydrogen atoms, observed and calculated structure factor amplitudes, Figs. S1–S3, and hydrogen coordinates, bond distances and angles, and magnetic data are available from the authors on request.

Acknowledgements

C.J.O. wishes to acknowledge support from grants from the Louisiana Education Quality Support Fund administered by the Board of Regents of the state of Louisiana and the donors of the Petroleum Research Fund administered by the American Chemical Society.

References

1 T. Mallah, O. Kahn, J. Gouteron, S. Jeannin and Y. Jeannin, *Inorg. Chem., 26* (1987) 1375.
2 V. McKee, M. Zvagulis, J. V. Dadgegian, M. G. Patch and C. A. Reed, *J. Am. Chem. Soc., 106* (1984) 4765.
3 T. Mallah, M. L. Boillet, O. Kahn, J. Gouteron, S. Jeannin and Y. Jeannin, *Inorg. Chem., 25* (1986) 3058.
4 E. E. Eduok and C. J. O'Connor, *Inorg. Chim. Acta, 88* (1984) 229.
5 C. J. O'Connor, D. A. Firmin, A. K. Pant, B. Ram babu and E. D. Stevens, *Inorg. Chem., 25* (1986) 2300.
6 M. T. Boillot, O. Kahn, C. J. O'Connor, J. Gouteron, S. Jeannin and Y. Jeannin, *J. Chem. Soc., Chem. Commun.,* (1985) 178.
7 T. Mallah, M. L. Boillot, O. Kahn, J. Gouteron, S. Jeannin and Y. Jeannin, *Inorg. Chem., 25* (1986) 3058.
8 T. N. Sorrell, C. J. O'Connor, O. P. Anderson and J. H. Rubenspies, *J. Am. Chem. Soc., 107* (1985) 4199.
9 O. Kahn, T. Mallah, J. Gouteron and Y. Jeannin, *J. Chem. Soc., Dalton Trans.,* in press.
10 W. P. J. Gajkema, W. G. J. Hal. J. M. Vereiken, N. M. Salter, H. J. Bah and J. J. Beintema, *Nature (London), 309* (1984) 23.
11 J. Larosche, W. Haase and P. V. Huong, *Inorg. Biochem., 27* (1986) 53.
12 E. I. Salomon, in T. G. Spiro (ed.), *Copper Proteins,* Wiley, New York, 1981, Ch. 1.
13 C. J. O'Connor, *Prog. Inorg. Chem., 29* (1982) 203.
14 P. Main, S. J. Fishe, S. E. Hull, L. Lessinger, G. Germaine, J. P. Declereq and M. M. Woolfson, *MULTAN 80,* a system of computer programs for the automatic solution of crystal structures from X-ray diffraction data, Universities of York, U.K. and Louvain, Belgium, 1980.
15 B. A. Frenz, in H. Schenk, R. Olthof-Hazekamp, H. van Koningsveld and G. G. Bassiz (eds.), *Computing in Crystallography,* Delft University Press, Delft, 1987.
16 *International Tables for X-ray Crystallography,* Vol. IV, Kynoch, Birmingham, U.K., 1974.
17 R. J. Majeste, C. L. Klein and E. D. Stevens, *Acta Crystallogr., Sect. C, 39* (1983) 52.
18 A. P. Ginsberg, R. L. Martin, R. W. Brookes and R. C. Scherwood, *Inorg. Chem., 11* (1972) 2884.